COMPUTER SIMULATION OF POSITIVE STREAMER DYNAMICS IN STRONGLY NON-UNIFORM ELECTRIC FIELDS IN AIR. EFFECT OF APPLIED VOLTAGE ON A STREAMER VELOCITY FOR DIFFERENT NEEDLE RADII

O.V. Manuilenko, V.I. Golota

NSC "Kharkov Institute of Physics and Technology", Kharkov, Ukraine

E-mail: ovm@kipt.kharkov.ua

The results of numerical simulations of the propagation of a positive streamer in air are presented. The positive streamer dynamics in the strongly non-uniform electric fields in air was investigated for wide set of applied voltages and needle radii. It is shown that qualitatively the dynamics of positive streamer in air does not differ from the negative streamer dynamics in nitrogen. Namely, streamer velocity has the same behavior in time during propagation in discharge gap, and the same trends with applied voltage increase and with decrease of needle radius.

PACS: 52.80.Mg, 52.80.Tn

INTRODUCTION

A systematic study of the influence of radius of the needle on the speed of the positive streamer (PS) is conducted in [1]. But in [1] the simulations were done for different needle radii, and just for single case of applied voltage. In the present paper the PS dynamics in the strongly non-uniform electric fields in air was investigated for wide set of applied voltages and needle radii. It is shown that qualitatively the PS dynamics in air does not differ from the negative streamer (NS) dynamics in nitrogen [2, 3]. Namely, streamer velocity has the same behavior in time during propagation in discharge gap-a sharp drop at the beginning of the movement, a propagation with nearly constant velocity, a region of the first (low) acceleration, and a region of the second (strong) acceleration at the approach of the streamer head to the anode. The PS velocity has the same trends with increase of applied voltage and with decrease of needle radius-the PS velocity increases with applied voltage, and with decreasing radius of the needle. The growth of the PS speed, with decreasing of the needle radius, is stopped when the needle curvature radius reaches a certain critical value.

1. MODEL

The simulation model for the PS dynamics in air is discussed in [1]. It consists from the coupled continuity equations (in the drift-diffusion approximation) for densities of electrons, positive ions, negative ions, and Poisson equation for electric field potential. The collisional ionization, photoionization, attachment, electron-ion recombination, and ion-ion recombination are included in the model. Fig. 1 shows the simulation domain and boundary conditions. Initially, particles are located at the anode with densities: $n_{e,p,n} = \delta_{e,p,n} \exp\left(-r^2/\sigma_r - (z-L_z)^2/\sigma_z\right)$, δ_e = 9·10^{13} cm^{-3}, δ_p = 1·10^{14} cm^{-3}, δ_n = 1·10^{13} cm^{-3}, σ_r = 1·10^{-4} cm^2, σ_z = 6.25·10^{-4} cm^2 , subscript e means electrons, p − positive ions, n − ntgative ions. Anode voltages are V_0 = {8, 10, 12, 15} kV, L_z = 2 mm, L_r =0.5 mm, needle radius is one of R ={0.25, 0.5, 1.0, 2.0}$\cdot H_{ndl}$, needle height is H_{ndl}=0.3125 mm. In the case of plane - to - plane geometry $R + H_{ndl}$=0.

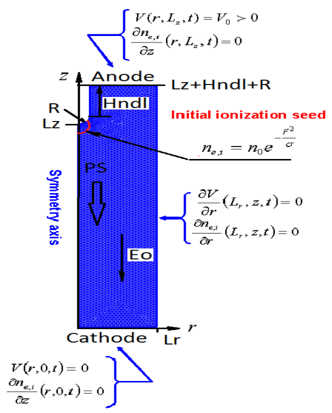

Fig. 1. Simulation domain and boundary conditions

2. UNIFORM ELECTRIC FIELDS

Fig. 2 shows the dynamics of PS in the homogeneous fields for V_0 =12 kV, which corresponds to the Laplacian (vacuum) electric field of 60 kV/cm. The initial conditions are chosen to avoid the avalanche stage, when the Laplacian electric field is not disturbed by the generated space charge field − $\delta_{e,p} \propto 10^{14}$ cm^{-3}. Fig. 2 shows distribution of the space charge density $\rho(r,z;t)$ in $\{r,z\}$ at different times. The arrows in Fig. 2 shows the electric field $\vec{E}(r,z;t)$. After a short initial stage (< 1·10^{-10} s), a PS is formed. It moves in the direction of the applied Laplacian field. For t > 1·10^{-9} s the electric field is substantially enhanced in front of the PS head, and attenuated behind it. After an initial rise, the electric field in front of the PS head slightly decreases as it moves toward the cathode, and then increases when the head of the PS approaches the cathode (also Fig. 3). It is clear from Fig. 2 that after the formation of the PS head, the streamer radius first decreases and then increases as it moves to the cathode, creating a constriction on the body of the PS.

Fig. 3 shows the electric field $|\vec{E}(r=0,z;t)|$ on the axis at different times. After a rapid rise in the initial stage, the electric field at the PS head decrease. When the PS head approaches the cathode, the local electric field in front of the streamer head is increased. This leads to the growing impact ionization rate and the rate of photoionization. This, in turn, leads to an increase in the densities of charged particles, and the rise of the space charge density. As the PS moves to the cathode, its head is broadened in the longitudinal direction, which is associated with the presence of photoionization. It is clearly seen from the space charge density distributions at different times (see Fig. 2). This behavior differs from the movement of the NS in nitrogen [2, 3], where there is no photoionization, and the NS head, as it moves towards the anode, shrinks and increases in magnitude.

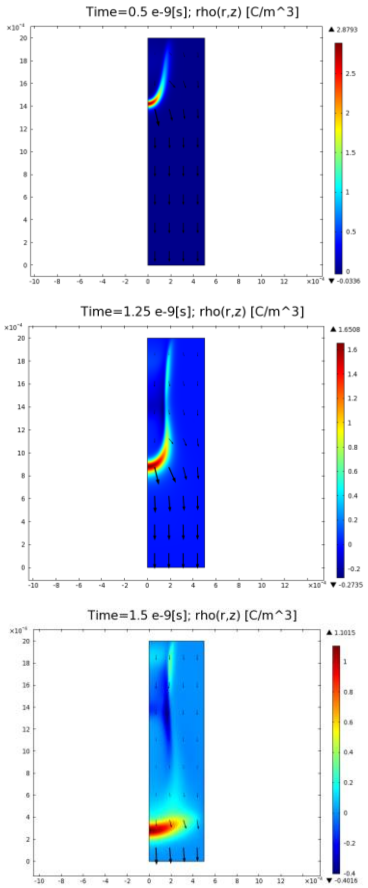

Fig. 2. Space charge density $\rho(r,z;t)$

Fig. 4 shows the velocity of $|\vec{E}(r=0,z;t)|^{max}$ versus time, which is the PS velocity – $V_s(t)$ for V_0 = {8, 10, 12, 15} kV. The behavior of the velocity has, as in the case of NS in nitrogen [2, 3], the characteristic regions: the sharp drop of the velocity at the beginning of the movement, the propagation with nearly constant velocity, the area of the first (low) acceleration, and the region of the second (strong) acceleration at the approach of the streamer head to the cathode. In contrast to the NS [2, 3], the region of constant velocity can not be identified as the initial linear stage of the avalanche, when the space charge is small, and the external electric field is practically not distorted by it.

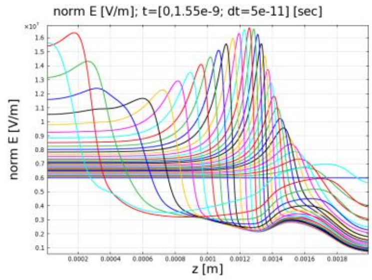

Fig. 3. Electric field $|\vec{E}(r=0,z;t)|$ *at different times*

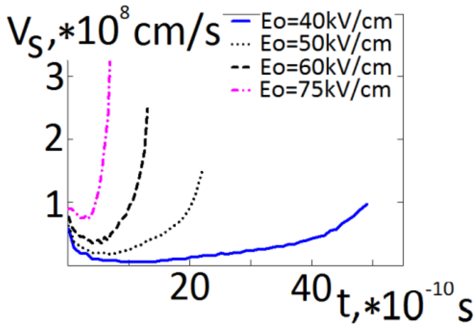

Fig. 4. Streamer velocity $V_s(t)$ *versus time*

3. NON-UNIFORM ELECTRIC FIELDS

Fig. 5 shows, as an example, the simulation results of the PS propagation through the discharge gap with non-uniform electric fields. V_0 =12 kV, R = 0.25·Hndl. The initial and boundary conditions are the same as in Section 3. Fig. 5 presents the space charge density $\rho(r,z;t)$ at different times. The arrows indicate the electric field. The dynamics of the streamer passage through the discharge gap is changed in comparison with the case of the uniform field. These changes are due to increased Laplacian electric field on the needle and the appearance of the radial electric field. The increased Laplacian electric field on the tip causes movement of the streamer, at least at the initial stage, in higher fields as compared with the plane-to-plane case. Which in turn, leads to an increase in its speed (Figs. 6, 7), and a decrease the time of the streamer formation. The radial electric field increases the transverse dimension of the streamer in comparison with the plane - to - plane case.

After a short initial stage (< $1\cdot10^{-10}$ s), a PS is formed. For t > $1\cdot10^{-9}$ s the electric field is enhanced in front of the PS head, and attenuated behind it. After an initial growth, the electric field in front of the PS head decreases as it moves through the discharge gap, and then increases when the head of PS comes close to the cathode. It is clear from the Fig. 5 that after the formation of the PS head, the radius first decreases and then increases as it moves to the cathode, creating a constriction on the body of the streamer. As in the plane case, the generation of the electrons due to photoionization has a maximum in the vicinity of the streamer head, where is maximal impact ionization. Photoionization region is always wider than the area of impact ionization, which leads to the birth of the electrons in front of the PS head.

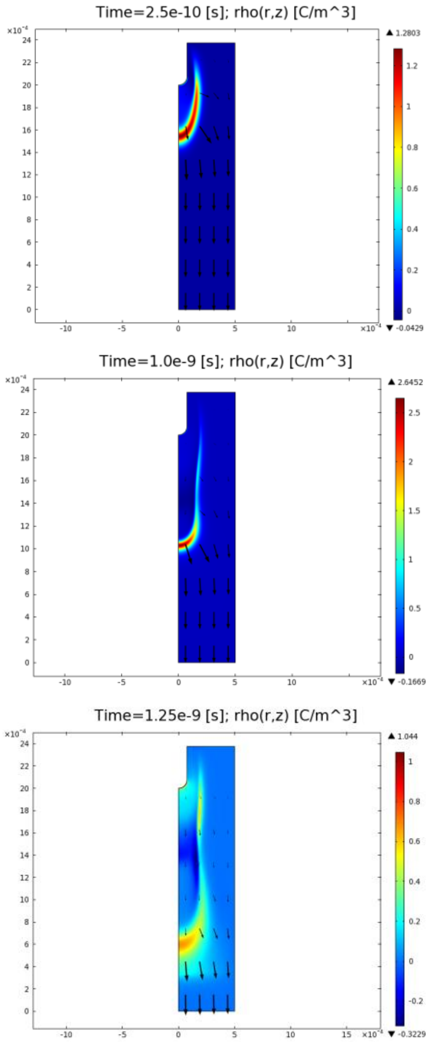

Fig. 5. Space charge density $\rho(r,z;t)$

Fig. 6 shows the PS velocities $V_s(t)$ for different values of the needle radii R = {0.25, 0.5, 1.0, 2.0, inf}$\cdot H_{ndl}$ at anode potential V_0 = {10, 12} kV. The R = inf means uniform electric field. As seen from Fig. 6, the PS velocity versus time $V_s(t)$ behaves as a speed of the NS in nitrogen [2, 3]. There are four characteristic regions: the sharp drop of the velocity at the beginning of the movement, the propagation with a nearly constant velocity, the area of the first (weak) acceleration, and the region of the second (strong) acceleration at the approach of the PS head to the cathode. As seen from Fig. 6, the PS velocity increases with decreasing radius of curvature of the needle at a predetermined potential on the anode. This increase in the velocity goes up to a certain radius (in this case R = 0.5$\cdot H_{ndl}$), after which the growth of the PS speed is cuted off. It is also seen that the velocity in a non-uniform field is higher than the speed in an uniform field. Fig. 7 shows the PS velocities $V_s(t)$ for different applied voltages V_0 = {8, 10, 12} kV at constant needle radii R = {0.25, 2.0}$\cdot H_{ndl}$. As seen from Fig. 7, the PS velocity increases with increase applied voltages.

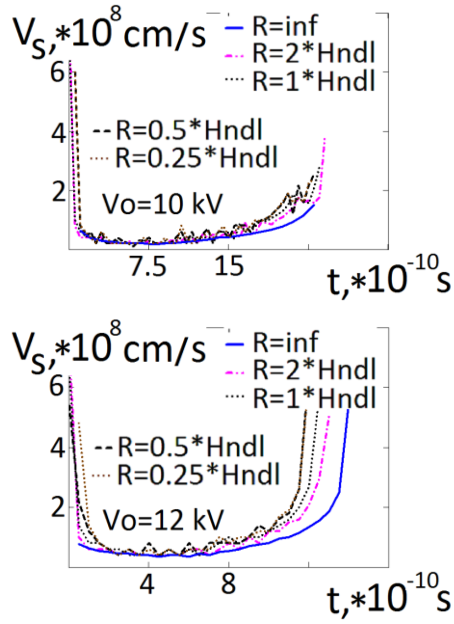

Fig. 6. PS velocity vs time for different needle radii

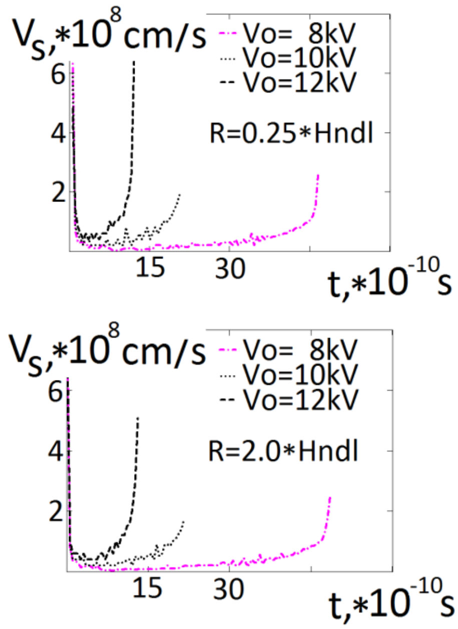

Fig. 7. PS velocity vs time for different applied voltages

Fig. 8 shows the PS mean velocity $<V_s>$ as a function of the needle radius. $<V_s>$ is defined as $<V_s> = L_z/\tau_{tr}$, where L_z is the discharge gap length, τ_{tr} is the passage time of the streamer through the discharge gap. It can be seen that the $<V_s>$ slightly increases with decreasing R. Starting from some R, the growth of the speed stops. Fig. 9 shows the $<V_s>$ as a function of the applied voltage for different needle radii. It can be seen that the $<V_s>$ increases approximately linearly with applied voltage.

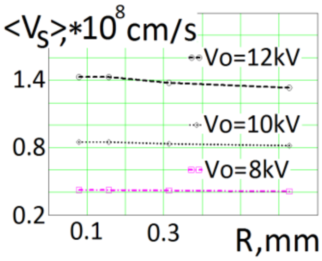

Fig. 8. $<V_s>$ *vs radius of the needle* R

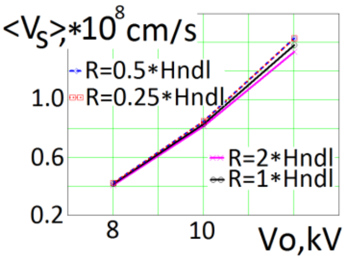

Fig. 9. $<V_s>$ *vs applied voltage* V_0

CONCLUSIONS

The results of numerical simulations of the propagation of a positive streamer in the atmospheric pressure air in the uniform and strongly non - uniform electric fields are presented. It is shown that the velocity of the positive streamer versus time behaves as a speed of the negative streamer in nitrogen [2, 3]. There are four characteristic regions: the sharp drop of the velocity at the beginning of the movement, the propagation with a nearly constant velocity, the area of the first (low) acceleration, and the region of the second (strong) acceleration at the approach of the streamer head to the cathode.

It is shown that the propagation velocity of the positive streamer in a non – uniform electric field is higher than its velocity in an uniform field at given voltages on electrodes. It is shown that with decreasing needle radius velocity of the streamer is increased at given voltages on electrodes. This growth continues until a critical radius, after which the growth of the positive streamer velocity practically stops. It is shown that with increasing applied voltage the streamer speed is increased.

REFERENCES

1. O.V. Manuilenko. Computer simulation of positive streamer dynamics in uniform and non-uniform electric fields in air // *Problems of Atomic Science and Technology. Ser. "Plasma Electronics and New Meth. of Accel." (8).* 2013, № 4, p. 194-199.
2. O.V. Manuilenko, V.I. Golota. Particularities of the negative streamer propagation in homogeneous and inhomogeneous electric fields, Computer simulation // *Problems of Atomic Science and Technology. Ser. "Plasma Physics" (19).* 2013, № 1, p. 171-173.
3. O.V. Manuilenko, V.I. Golota. Numerical simulation of negative streamers in strong non-uniform electric fields in nitrogen. Effect of needles radius and applied voltage on streamer velocity // *Problems of Atomic Science and Technology. Ser. "Plasma Electronics and New Meth. of Accel." (8).* 2013, № 4, p. 189-193.

Article received 22.10.2014

КОМПЬЮТЕРНОЕ МОДЕЛИРОВАНИЕ ДИНАМИКИ ПОЛОЖИТЕЛЬНЫХ СТРИМЕРОВ В СИЛЬНО НЕОДНОРОДНЫХ ЭЛЕКТРИЧЕСКИХ ПОЛЯХ В ВОЗДУХЕ. ВЛИЯНИЕ ПРИЛОЖЕННОГО НАПРЯЖЕНИЯ НА СКОРОСТЬ СТРИМЕРА ДЛЯ РАЗЛИЧНЫХ РАДИУСОВ ИГЛЫ

О.В. Мануйленко, В.И. Голота

Представлены результаты численного моделирования распространения положительного стримера в воздухе. Динамика положительного стримера в сильно неоднородных электрических полях исследована для широкого набора приложенных напряжений и радиусов иглы. Показано, что качественно динамика положительного стримера в воздухе не отличается от динамики отрицательного стримера в азоте. А именно, скорость положительного стримера в воздухе при распространении через разрядный промежуток ведет себя во времени так же, как и скорость отрицательного стримера в азоте, кроме того, скорость стримера увеличивается с увеличением приложенного напряжения и с уменьшением радиуса иглы.

КОМП'ЮТЕРНЕ МОДЕЛЮВАННЯ ДИНАМІКИ ПОЗИТИВНИХ СТРИМЕРІВ У СИЛЬНО НЕОДНОРІДНИХ ЕЛЕКТРИЧНИХ ПОЛЯХ У ПОВІТРІ. ВПЛИВ ПРИКЛАДЕНОЇ НАПРУГИ НА ШВИДКІСТЬ СТРИМЕРА ДЛЯ РІЗНИХ РАДІУСІВ ГОЛКИ

О.В. Мануйленко, В.І. Голота

Представлено результати числового моделювання поширення позитивного стримера в повітрі. Динаміка позитивного стримера в сильно неоднорідних електричних полях досліджена для широкого набору прикладених напруг і радіусів голки. Показано, що якісно динаміка позитивного стримера в повітрі не відрізняється від динаміки негативного стримера в азоті. А саме, швидкість позитивного стримера в повітрі, при поширенні через розрядний проміжок поводиться у часі подібно до швидкості негативного стримера в азоті, крім того, швидкість стримера збільшується зі збільшенням прикладеної напруги і зі зменшенням радіусу голки.